Efficient Image Dataset Classification Difficulty Estimation for Predicting Deep-Learning Accuracy

Florian Scheidegger*†, Roxana Istrate‡†, Giovanni Mariani†
Luca Benini*§, Costas Bekas†, Cristiano Malossi†
*ETH Zürich, Switzerland †IBM Research - Zürich, Switzerland
‡Queen's University of Belfast, United Kingdom §Università di Bologna, Italy

Abstract—**In the deep-learning community new algorithms are published at an incredible pace. Therefore, solving an image classification problem for new datasets becomes a challenging task, as it requires to re-evaluate published algorithms and their different configurations in order to find a close to optimal classifier. To facilitate this process, before biasing our decision towards a class of neural networks or running an expensive search over the network space, we propose to estimate the classification difficulty of the dataset. Our method computes a single number that characterizes the dataset difficulty $27\times$ faster than training state-of-the-art networks. The proposed method can be used in combination with network topology and hyper-parameter search optimizers to efficiently drive the search towards promising neural-network configurations.**

I. INTRODUCTION

Convolutional Neural Networks (CNNs) gained popularity in recent years thanks to the availability of powerful GPUs that enable to efficiently train accurate classification models [1]. For building practical applications, the deep-learning community shares a common interest in reducing the development cycle, while increasing model accuracy and keeping infrastructure and power consumption expenditure under control. Many publications address these conflicting goals [2], [3], [4]. Most machine-learning approaches require a human in the loop responsible for taking crucial decisions such as defining the network, finding good combinations of hyper-parameters and performing adequate preprocessing on the input data. To overcome the problem of manual selection various automated approaches such as Grid Search, Random Search [5], Bayesian optimization [6] or Hyperband optimization [7] have been proposed. These

methods operate autonomously and improve model performance, however they still have two limiting factors. First, they require a definition of the search space. Second, they consume a large amount of resources for a single optimization task.

In this paper we propose automated methods for quantifying the *difficulty* of a classification problem in terms of how hard it is to reach high accuracy for a given dataset. The proposed method can be used in combination with architecture search optimizers to efficiently drive the search towards promising configurations, avoiding the exploration of unsuitable networks. Consciously or not, the characterization of dataset difficulty is a process followed by every deep learning architect. When looking for a well-performing model for a new dataset, common practice is to try state-of-the-art networks to evaluate how hard is to classify the images in the dataset. Since datasets are large and models complex, the process of training, comparing, and selecting a few state-of-the-art deep networks becomes a computationally heavy task. We propose to optimize this step by providing a classification difficulty estimator, that provides insights into the classification task and can be used to rapidly confine the exploration to a few promising networks. We aim to construct dataset characterizations that run orders of magnitude faster than the actual training and have high correlation with state-of-the-art network accuracies.

In summary, our main contributions are the following:

- We propose and evaluate three different dataset complexity scoring pipelines.
- We conduct various deep learning experiments with fixed hyper-parameter and data augmentation configurations that run on thirteen datasets.
- We evaluate approximate computing techniques, such as subsampling and early stopping, in order to reduce the execution time without affecting the end results.

The remainder of the paper is organized as follows. Section II describes the related work, Section III introduces the notation used throughout the paper, Section IV details the adopted methodologies, Section V examines the results, and Section VI concludes the current work.

II. RELATED WORK

The topic of difficulty estimation of a dataset is scarcely explored in the literature. In [8], the authors address this problem by using, but use as reference the human response time for solving a visual search task. As compared to our technique which focuses on defining how easily separable are the different classes in a dataset, their technique analyses a dataset difficulty on an image based approach and employs two VGG-like [9] networks that work as encoders and extract features that are further passed through a regressor. The complexity of this solution comes from passing the full dataset through the VGG-like networks, since the VGG family includes one of the largest state-of-the-art network with 138M parameters and 15 GFLOPs/inference.

Figure 1 shows state-of-the-art accuracies achieved by thirteen of the most commonly used image classification datasets: *MNIST* [10], *GTSRB* [11], *svhn* [12], *CIFAR10* [13], *flowers*[1], *flowers102* [14], *fashion MNIST* [15], *food101* [16], *CIFAR100* [13], *stl10* [17], *textures* [18], *indoor67* [19], and *places* [20]. As expected, more results are available for the highly curated datasets, such as *MNIST* and *CIFAR10/100*. The same holds for datasets introduced as part of a competition, such as the German Traffic Sign Recognition Benchmark (*GTSRB*), where the authors published the full performance list of over a hundred machine learning algorithms. For less popular datasets, results are harder to acquire. In this category fits the flowers dataset, which was introduced in a tensorflow tutorial[2] with the purpose of explaining transfer learning. In that case, transferred learning [21] provides superior classification performance over any CNN trained from scratch. General embeddings obtained from pretrained models help increasing performance for a specific task, especially when the data is limited [22]. Figure 1 reveals that all mentioned algorithms, even non-CNN based ones, easily reach accuracies above 95% on *MNIST*. This observation motivated the authors of *fashion MNIST* to introduce a more diverse dataset in terms of images, but equal to *MNIST* in terms of number

---

[1] Available at http://download.tensorflow.org/example_images/flower_photos.tgz

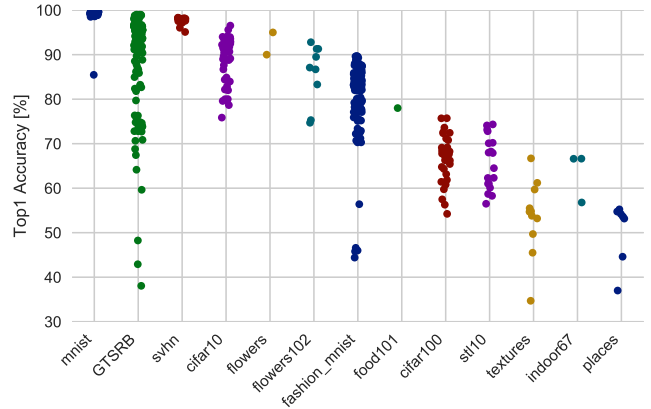[2] Available at https://www.tensorflow.org/tutorials/image_retraining

Fig. 1. State-of-the-art results achieved on various datasets. Each point corresponds to a single published algorithm. For well established datasets, or for datasets that were part of a public challenge, many Top1 results are known. The picture combines vanilla CNNs with or without transfer learning, non-deep learning approaches such as SVMs or Random Forests applied on handcrafted features, and other problem specific pipelines.

of training/validation samples, image sizes and number of classes. This allows any algorithm designed for *MNIST* to run without modification on *fashion MNIST*. Their initial study demonstrates a wider spread in performance among different algorithms and consistently lower performance when compared with the same algorithms evaluated on *MNIST* [15].

To the best of our knowledge, there is no published work that focuses on automatically ranking classification difficulty among datasets.

III. NOTATION

In this work, we refer to a dataset with the quadruple $\mathcal{D} := (\mathbf{X}_{train}, \mathbf{y}_{train}, \mathbf{X}_{test}, \mathbf{y}_{test})$, where $\mathbf{X}_{train} \in \mathbb{R}^{n_{train} \times d}$ and $\mathbf{X}_{test} \in \mathbb{R}^{n_{test} \times d}$ are the training and testing inputs, and $\mathbf{y}_{train} \in [1, C]^{n_{train}}$ and $\mathbf{y}_{test} \in [1, C]^{n_{test}}$ are the training and testing labels. We assume that the datasets come already split into train and test sets, as this is commonly the case for published data. We denote the input dimension as d, the number of input samples as n_{train} for training and n_{test} for testing, and the number of classes as C. $\mathcal{M}$ refers to a model, including the network topology and related hyper-parameters, and it includes the training and data augmentation related hyper-parameters. Therefore, the tuple $(\mathcal{D}, \mathcal{M})$ specifies a deep learning training run of model $\mathcal{M}$ on dataset $\mathcal{D}$. We denote with Top-1$(\mathcal{D}, \mathcal{M})$ the Top-1 accuracy classification performance of the training run. In all

Score	Transformation	$\bar{d}$	Distance	Speedup
S_1	None	d	MSE	$31.3\times$
S_2	None	d	DSSIM	1.0 (Ref)
S_3	Resize image	8^2	MSE	$48.4\times$
S_4	Resize image	8^2	DSSIM	$1.3\times$
S_5	PCA	10	MSE	$72.8\times$
S_6	Autoencoder	1000	MSE	$6.4\times$

experiments, training is performed with $(\mathbf{X}_{train}, \mathbf{y}_{train})$ and performance is measured on $(\mathbf{X}_{test}, \mathbf{y}_{test})$.

IV. RANKING DATASETS

In this work we proposed metrics to quantify the *difficulty* of image classification datasets. We propose dataset scoring functions $r(\mathcal{D})$ to map a dataset $\mathcal{D}$ to a scalar real number with the goal of ranking different datasets in terms of classification accuracy estimates.

A. Silhouette Score

The silhouette score is a well established metric that compares tightness of same-class samples to separation of different-class samples [23]. Let i be one input sample, $a(i)$ the average euclidean distance between the sample and all the points j belonging to the same class as i, and $b(i)$ the average distance between i and all points j of the closest different class. The *silhouette* of the i-th sample is computed [23] as follows:

$$s(i) := \begin{cases} 1 - a(i)/b(i), & \text{if } a(i) < b(i) \\ 0, & \text{if } a(i) = b(i) \\ b(i)/a(i) - 1, & \text{if } a(i) > b(i). \end{cases} \quad (1)$$

The silhouette of one class is defined as the average over all samples belonging to that class and the overall silhouette score of the full dataset is defined as average over all samples. The definition of the quantities $a(i)$ and $b(i)$ are based on pairwise distances between two samples i and j. The silhouette score complexity is $O(\bar{d}n^2)$, where n is the number of samples and $\bar{d}$ is the cost of computing the distance of one pair of samples as mean squared error (MSE) distance in the $\mathbb{R}^{\bar{d}}$. Since, the MSE distance in the original domain is a poor measurement for image similarities, we apply first a transformation $\mathbb{R}^d \to \mathbb{R}^{\bar{d}}$ that maps images into a space that better reflects distances between image pairs.

Table I provides details on the applied pipelines. We decided to include a resizeing of the images to a small resolution of 8×8 pixels, applying principal component analysis (PCA) to reduce the dimension to 10, and using a fixed encoding based on a pretrained CNN inference. We considered as encoder a ResNet-50 [24] network pretrained on ImageNet [25] to produce generalized per image feature vectors of dimensionality 1000 by taking the output of the last fully connected layer before applying the non-linearity. Additional to the MSE distance, we used the structural dissimilarity index DSSIM [26] to compare images with a metric that captures spatial information. Due the squared complexity, we applied heavy subsampling and run all computations with a maximum of 1000 randomly selected samples, resulting in a distance matrix with at most $1M$ entries. Table I states timing among the different pipelines. For fast execution, it is crutial to operate in a low dimensional space and to use a simple distance metric.

B. K-means Clustering

The complexity of the silhouette scores detailed in Subsection IV-A scales with n^2, and computing it is a slow process even after subsampling. In general, the complexity of a deep-learning job is $O(c(\mathcal{M})n_{train}e))$, where e is the number of epochs. During one epoch the full training set consisting of n_{train} samples is fed once with a computational cost of $c(\mathcal{M})$, where $c(\mathcal{M})$ is a model dependent constant. Even though complex models might have large computational cost of $c(\mathcal{M})$, the asymptotic behaviour of a training job is linear in n. For this reason, the asymptotic behaviour of the silhouette score computation of n^2 is outperformed by the actual training job. Competitive scoring metrics should execute faster than a train job itself, thus we are looking for scores with at most linear complexity in n.

We propose to run a (fast) clustering algorithm to produce class labels $\tilde{\mathbf{y}}$ and evaluate the full dataset based on metrics that compare $\tilde{\mathbf{y}}$ against the ground truth labels $\mathbf{y}$. We assess the following known scores: adjusted mutual information [27], adjusted rand index [28], completeness, homogeneity and the v-measure [29]. Additionally, we propose an own tailored score based on the estimation of the confusion matrix built between the cluster indices and the true labels. Clustering algorithms work in an unsupervised fashion, meaning that the clusters are not assigned to any label. To estimate the confusion matrix we require an one-to-one mapping between the clusters and the labels. A naïve solution computes all possible permutations, and selects the one that maximizes the

a)
32x32x3
CONV, 8 (2) [32]
16x16x8
CONV, 16 (4) [64]
8x8x16
CONV, 32 (8) [128]
4x4x32
C - way Softmax

b)
32x32x3
3x3 CONV, 8 (2)
16x16x8
C - way Softmax

c)
32x32x3
CONV, 8 (32)
16x16x8 (16x16x32)
CONV, 16 (64)
8x8x16 (8x8x64)
CONV, 32 (128)
4x4x32 (4x4x128)
CONV, 64 (256)
2x2x64 (2x2x256)
CONV, 128 (512)
1x1x128 (1x1x512)
C - way Softmax

d)
32x32x3
DENSE, 3/4*1024+1/4*C
DENSE, 2/4*1024+2/4*C
DENSE, 1/4*1024+3/4*C
C - way Softmax

e)
32x32x3
CONV, 8*log10(C)
CONV, 4*sqrt(C)
CONV, C
DENSE, 2*C
C - way Softmax

f)
32x32x3
Chained CONVs, r=log(C), f=8
16x16x8
Chained CONVs, r=log(C), f=16
8x8x16
Chained CONVs, r=log(C), f=32
4x4x32
Chained CONVs, r=log(C), f=64
2x2x64
Chained CONVs, r=log(C), f=128
1x1x128
DENSE, (512+C)/2
C - way Softmax
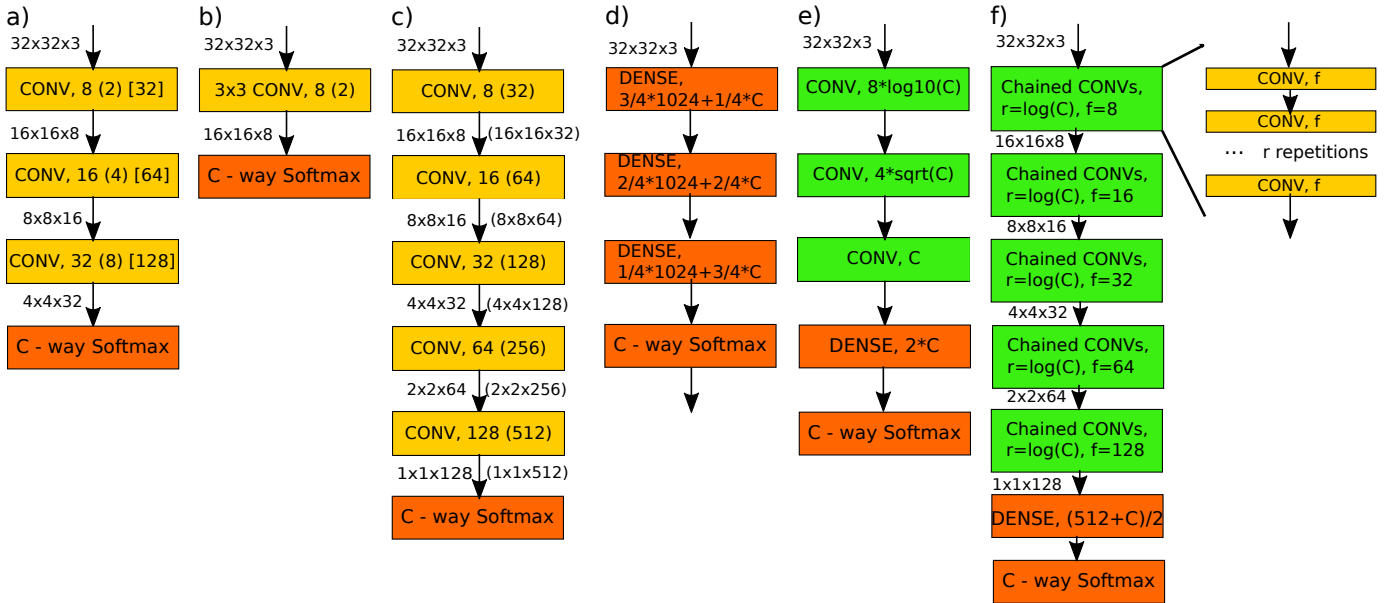
CONV, f
CONV, f
··· r repetitions
CONV, f

Fig. 2. *Probe nets*: simple deep learning architectures used to characterize datasets. *Static* networks are shown in Subfigure a), b) and c), they only differ in the dense layer connections in the softmax output that ends with a dataset specific number of classes C. Subfigure a) shows a *regular*, *narrow* and *wide* probe net that differ in kernel depth, b) shows a *shallow* version and c) a *deep* version of the net for non and *normalized* kernel depths. *Dynamic* networks, d), e) and f), scale the topology with respect to the number of classes C. Subfigure d) consists of dense layers that scale the number of hidden units according to linear weighted sum between input and output dimension, Subfigure e) scales kernel depths according to C and Subfigure f) scales the number or repetions of stacked static layers according C.

trace normalized by the amount of total data points. Due to the factorial complexity, we propose to compute an approximate estimate with the following greedy algorithm. First, we search the maximum values per row and assign the clusters to the corresponding label. If the greedy strategy resolves to a bijective mapping, the accuracy is computed based on the found confusion matrix. Otherwise, the non-bijective contradictions are solved with extensive search. Since this approach still results in a worst case factorial complexity, we set an maximum limit of contradictions to be solved by exhaustive search to seven, and solve other contradictions by assigning an initial permutation. Hence, the accuracy estimate is the maximum achieved over all values obtained with permutations on the remaining problematic locations. It turns out that the proposed procedure is stable and fast to evaluate and it builds a lower bound to the optimal value. In few cases our chosen maximum limit of seven contradictions was exceeded.

C. Probe Nets

As alternative scoring metric we also investigate the possibility of training a small predefined neural network and score the dataset based on its accuracy. We call this network a *probe network*. The probe net model $\mathcal{M}_{probe}$ must be general enough to be applied to any image clas-

TABLE II
OPERATION COUNT AND NUMBER OF PARAMETERS OF PROPOSED PROBE NETS

Probe Net	$C = 10$		$C = 100$	
	OPs	Weights	OPs	Weights
Regular	0.81M	11K	0.86M	57.5K
Narrow	0.09M	2K	0.10M	13K
Wide	10.34M	114K	10.52M	299K
Shallow	0.24M	21K	0.42M	205K
Shallow norm.	0.06M	5K	0.10M	51K
Deep	1.40M	100K	1.41M	112K
Deep norm.	19.76M	1576K	19.81M	1622K
MLPs	2.90M	2908K	3.10M	3107K
Kernel depth	0.53M	6K	4.56M	384K
Length	1.41M	118K	4.39M	338K
ResNet-20	40.55M	271K	40.56M	277K

sification task and considerably faster: $c(\mathcal{M}_{probe}) << c(\mathcal{M})$. Additionally, to further speedup the execution time we stop the training of the probe net after few epochs, before full convergence.

We propose to construct variations of two types of probe nets: *static probe nets* that have a fixed topology and *dynamic probe nets* that scale the topology according to the number of classes. The *regular probe*
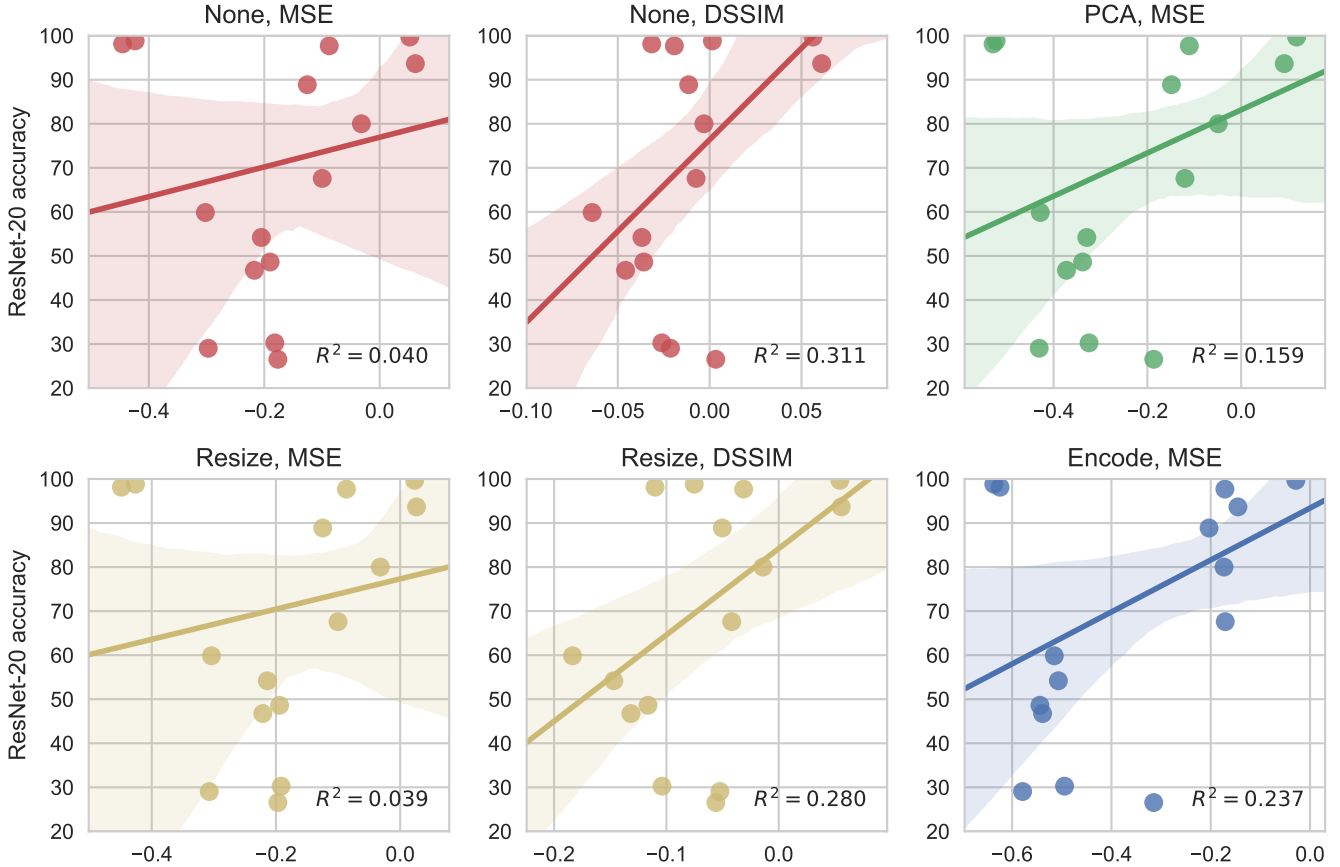
Fig. 3. Prediction performance of silhouette scores: the x-axis states variations of the silhouette scores according Table I and the y-axis states the model performance obtained by a state-of-the-art architecture, a ResNet-20 topology. Subfigures vary according pretransformation {None, Resize, PCA, Encode} and pairwise distance metrics {MSE, DSSIM}.

net consists of three convolutional layers, each followed by batch normalization, max pooling of size 2×2, and ReLU activations, which are defined element-wise as $x \mapsto \max(0, x)$. We used eight kernels in the first layer and doubled the number of kernels per layer. We provide *wide* and *narrow* variations that scale the number of kernels per layer up and down by $4\times$, respectively. *Shallow* and *deep* variations are obtained by subtracting and adding two layers, respectively. Since doubling the kernel sizes per layer leads to different tensor shapes between the last convolution and the C-way softmax, the *non-normalized shallow* and *deep probe nets* have a considerable different number of trainable parameters. We define *normalized probe networks* to match the number of trainable parameters of the output layer of the *regular probe net*. We construct *dynamic nets* with a more complex topology to account for more classes. This is achieved either by scaling dependent on C the number of hidden units in an multilayer percpetron *mlp*,

the number of filters (*filter depth scaled probe nets*), or the number of stacked filters (*length scaled probe net*). Figure 2 shows the ten proposed prob net architectures.

V. RESULTS

In order to perform a fair evaluation, we fix hyperparameters throughout the experiments. We use a ResNet-20 topology to compute the reference accuracy on all datasets resized to 32×32 pixels. We follow the data augmentation described in [30]. We use the RMSProp [31] optimizer to minimize the average cross entropy with a learning rate of 10^{-4}. All evaluations employ the He initialization [32] with a gain factor 1.0 and a constant batch size of 32. Training is run for 100 epochs. Results presented in Figure 3, Figure 4, and Figure 5 state the computed classification difficulty score on the x-axis plotted against the ResNet-20 accuracy reference that is shared among all plots. An ideal dataset

difficulty score should obey a linear dependency and match the reference accuracies.

A. Silhouette Score

Figure 3 compares the scores based on the proposed pipelines in Table I with the reference accuracies of a ResNet-20 [24]. The silhouette score based on the DSSIM pairwise distance outperforms the MSE based distance, as the former preserves spatial information of the image domain. Similarly, the (more expensive) computation with the full image domain slightly outperforms the resized counterpart, since it benefits from more information. Subfigure c) shows results when the silhouette score is applied on the PCA reduced space and in Subfigure f) the PCA is replaced by the autoencoder. Although reducing the dimensionality is often beneficial, we obtained the best correlation results with the DSSIM based distance on the original domain, with a weak correlation of $R^2 = 0.31$.

B. K-means Clustering

For the evaluation of the proposed k-means based scoring pipeline (see Subsection IV-B), we cluster the images in C clusters, where C is the knwon number of categories in the dataset. For a faster convergence, we initialize the centroids with the average image of each class. k-means runs based on the euclidean L_2 distance with a stopping tolerance of 10^{-4} and a maximum of 300 iterations without random restarts. Figure 4 shows the regression among proposed scores and the obtained reference accuracy of a ResNet-20.

Among columns different scores are assessed, such as the *accuracy on the estimated confusion matrix (AECM)*, the *adjusted mutual information* score, the *adjusted random score* and the *v-measure*. Results for the *homogeneity score* and the *completeness score* are omitted since they are highly correlated with the *v-measure*. Except the *v-measure* computed in the encoded setting, the scores are weakly positively correlated with the obtained ResNet-20 reference. Resizing to a small dimension of 8×8 only marginally affects results, applying PCA helps to improve predictions from around $R^2 = 0.25$ up to $R^2 = 0.31$. The encoder based pipeline provides an embedding that is in the same order of quality ($R^2 = 0.30$). Among the score computations the one based on AECM outperforms the other scores. The weak performance of the k-means clustering is due to known limitations, such as no global minimum guarantee and poor distance metric that ignores the spatial information. k-means clustering based pipelines are $5.2\times$ (no

pretransformation) up to $50.5\times$ (PCA pretransformation) faster than silhouette score based pipelines (comparison includes the faster MSE timings) when comparing execution times in terms of average per input sample.

C. Probe Nets

All proposed probe nets, as presented in Figure 2, are trained with the same constant configuration and data augmentation parameters as explained in Section V. Results are obtained after training for 100 epochs. Figure 5 shows all obtained correlations between runs of the ten proposed probe nets against the reference. All probe nets share a high correlation with the reference ResNet-20 of $R^2 > 0.88$ and consistently outperform results achieved with the k-means based approach, see Subsection V-B. Subfigure a) shows an increasing correlation of $R^2 = 0.89$ to $R^2 = 0.98$ between *narrow*, *regular*, and *wide* probe nets and the reference. This can be explained by the better generalization ability of the network with more degrees of freedom, at the cost of an increased execution time. For more details see Table II. *Deep* probe nets topologies outperform their *shallow* counterparts. This effect is even more prominent in the *normalized* case, Subfigure b) versus Subfigure d). We observe that a better generalization performance is mainly driven by a larger amount of tuneable parameters that comes at the cost of increased execution timings. Subfigures c) and e) of Figure 5 show the results for probe nets that dynamically adapt the architecture topology to the number of classes. The dependency of the architecture on the number of classes implies different execution times on datasets with different number of classes. The *mlp* can not compete with the CNN counterparts.

D. Efficient Evaluation of Probe Nets

As presented in Subsection V-C probe nets have a good predictive behaviour of what a reference network achieves on a given dataset. However, that information is only valuable if it can be computed order of magnitudes faster than training large models. The way probe nets are constructed give them an inherent computational benefit over the full model. In addition, we exploit early stopping of the learning to further reduce the computational time of the probe net. Note that we can stop the probe net before convergence, since we are interested in the learning trend that characterizes the problem's difficulty, not in the final accuracy. Figure 6 shows how the prediction quality improves for a regular probe net with an increasing amount of epochs for which
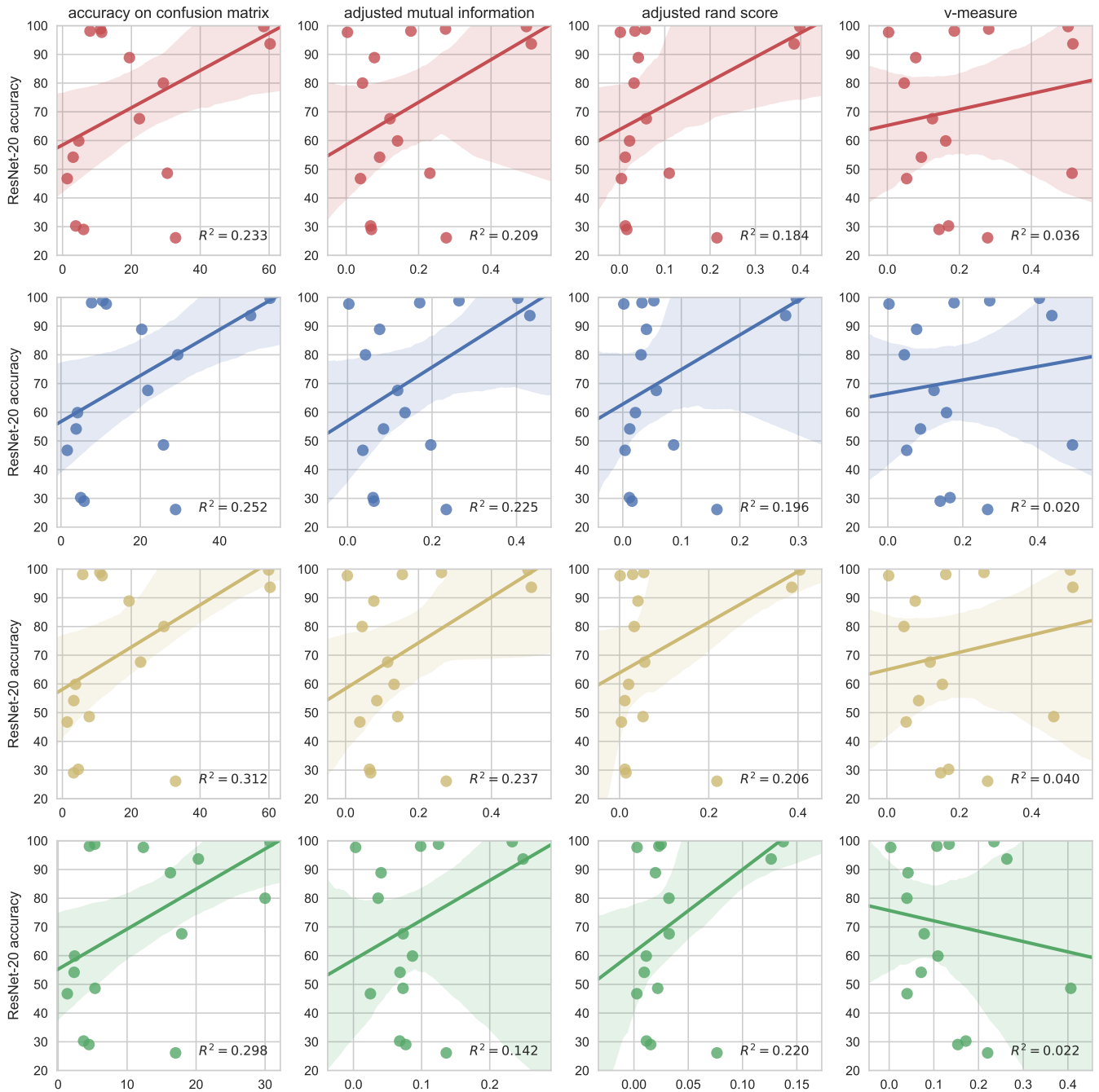
Fig. 4. Prediction performance of k-means based dataset scores: the x-axis states variations of the k-means based scores from Subsection IV-B and the y-axis states the model performance obtained by a state-of-the-art architecture, a ResNet-20 topology. Rows state results for applying none, resizing, PCA, and encoding as pretransformations. Columns state results for four metrics comparing the clustering with the ground truth classification. Scores based on the estimated confusion matrix outperform the others and applying PCA or an embedding is beneficial for accuracy prediction.

it is trained on all datasets. Within a few epochs the regression quality reaches a saturation at about $R^2 = 0.95$. The mean accuracy difference between the probe nets and the reference ResNets (trained till convergence) is

further decreased, meaning that the probe nets are not yet converged and are still increasing their own classification performance. Figure 6 highlights the achieved quality at epoch 1, 5 and 10. Figure 7 presents both intermediate
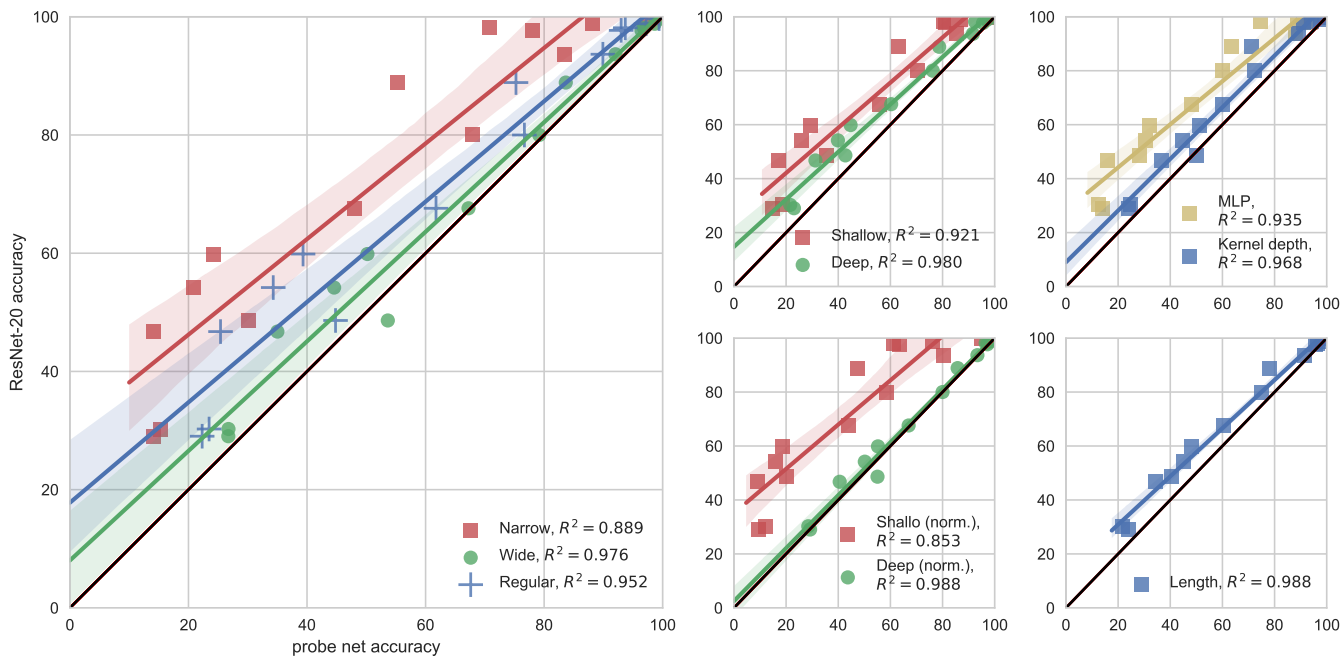
Fig. 5. Prediction performance of probe nets: the x-axis states the accuracy reached of a converged probe net and the y-axis states the model performance obtained by a state-of-the-art architecture, a Resnet-20 topology. All seven static probe nets, a) *regular/narrow/wide*, b) *shallow/deep*, c) *shallow/deep normalized*, and the three dynamic probe nets, d) *mlp*, *kernel depth* scaled, and e) *length* scaled are strongly correlated with results obtained with ResNet-20.

and after convergence results. With increasing number of epochs, the regression moves from the top-left corner towards the identity line in the middle. As few as 5 epochs are enough to reach the full dataset performance prediction ability, well before that actual probe net has converged.

VI. CONCLUSION

We formulated the question to compute a ranking among datasets that reflect their inherent classification difficulty. We suggested three processing pipelines, a silhouette based score, a k-means clustering based and a probe net based evaluation pipeline. The main drawback of the silhouette based approach is the high complexity, which scales with the squared number of samples. We proposed efficient score computing pipelines based on k-means and probe nets that scale linear in the number of samples. k-means delivers results one complexity class faster and with similar prediction quality as the silhouette approach, reaching a weak correlation with reference models of $R^2 = 0.31$. Finally, we presented the probe nets, which are small networks, and apply standard deep learning techniques in order to compute predictions that are strongly correlated with the reference from $R^2 = 0.89$ up to $R^2 = 0.99$. Even the worst performing probe

net outperforms silhouette and k-means based scoring with a wide quality margin. We further evaluated the fact of early stopping to reduce the data score evaluation time and observed little to no performance drop. Leveraging the small architectures of probe nets and early stopping allows to perform dataset scoring $27\times$ faster than the required training time of the actual reference model.

REFERENCES

[1] K. He, X. Zhang, S. Ren, and J. Sun, "Delving deep into rectifiers: Surpassing human-level performance on imagenet classification," in *Proceedings of the IEEE international conference on computer vision*, 2015, pp. 1026–1034.

[2] M. Courbariaux, I. Hubara, D. Soudry, R. El-Yaniv, and Y. Bengio, "Binarized neural networks: Training deep neural networks with weights and activations constrained to+ 1 or-1," *arXiv preprint arXiv:1602.02830*, 2016.

[3] S. Gupta, A. Agrawal, K. Gopalakrishnan, and P. Narayanan, "Deep learning with limited numerical precision," in *International Conference on Machine Learning*, 2015, pp. 1737–1746.
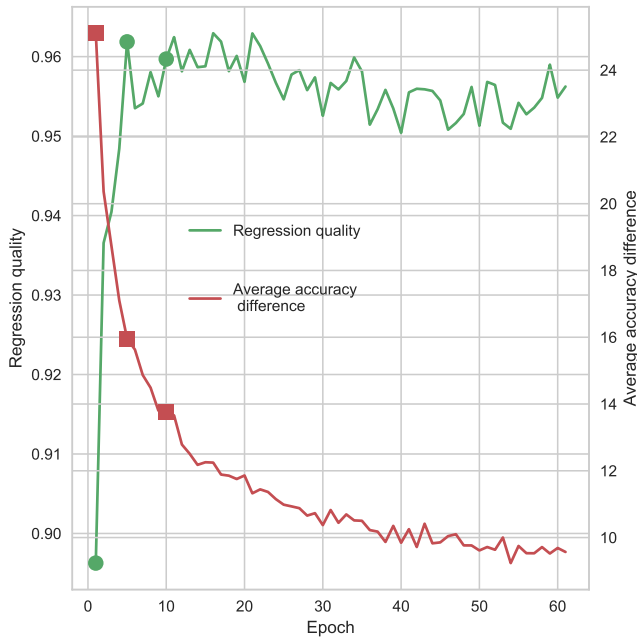
Fig. 6. Evolution of the prediction quality over training epochs of the *regular* probe net. The regression quality saturates around $R^2 = 0.96$ within a few epochs while the average accuracy difference between the probe net and the reference is further decreased for longer training.
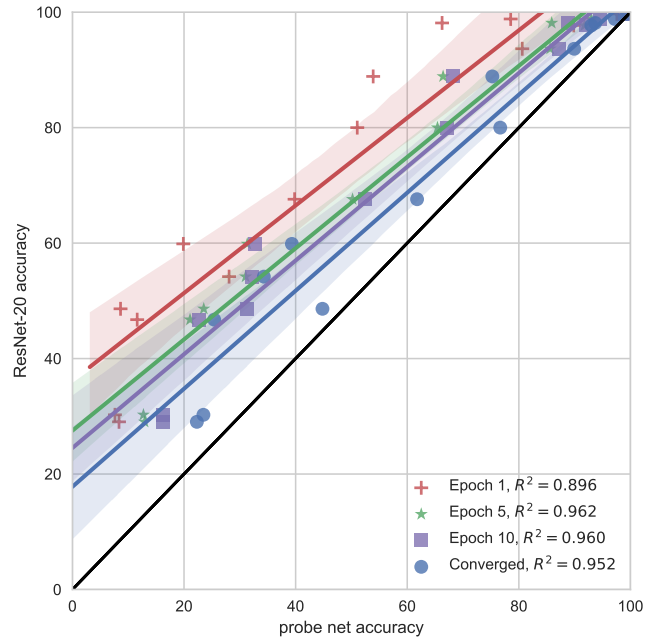

Fig. 7. Regression snap shots obtained at epoch 1, 5, 10 and at convergence of the *regular* probe nets.

[4] M. H. J. A. B. Hanzhang Hu, Debadeepta Dey, "Anytime neural network: a versatile trade-off between computation and accuracy," 2017.

[5] J. Bergstra and Y. Bengio, "Random search for hyper-parameter optimization," *Journal of Machine Learning Research*, vol. 13, no. Feb, pp. 281–305, 2012.

[6] J. Snoek, H. Larochelle, and R. P. Adams, "Practical bayesian optimization of machine learning algorithms," in *Advances in Neural Information Processing Systems 25*, F. Pereira, C. J. C. Burges, L. Bottou, and K. Q. Weinberger, Eds. Curran Associates, Inc., 2012, pp. 2951–2959. [Online]. Available: http://papers.nips.cc/paper/4522-practical-bayesian-optimization-of-machine-learning-algorithms.pdf

[7] L. Li, K. Jamieson, G. DeSalvo, A. Rostamizadeh, and A. Talwalkar, "Hyperband: Bandit-based configuration evaluation for hyperparameter optimization," 2016.

[8] R. Tudor Ionescu, B. Alexe, M. Leordeanu, M. Popescu, D. P. Papadopoulos, and V. Ferrari, "How hard can it be? estimating the difficulty of visual search in an image," in *Proceedings of the IEEE Conference on Computer Vision and Pattern Recognition*, 2016, pp. 2157–2166.

[9] K. Simonyan and A. Zisserman, "Very deep convolutional networks for large-scale image recognition," *arXiv preprint arXiv:1409.1556*, 2014.

[10] L. Deng, "The mnist database of handwritten digit images for machine learning research [best of the web]," *IEEE Signal Processing Magazine*, vol. 29, no. 6, pp. 141–142, 2012.

[11] J. Stallkamp, M. Schlipsing, J. Salmen, and C. Igel, "The german traffic sign recognition benchmark: A multi-class classification competition," in *The 2011 International Joint Conference on Neural Networks*, July 2011, pp. 1453–1460.

[12] Y. Netzer, T. Wang, A. Coates, A. Bissacco, B. Wu, and A. Y. Ng, "Reading digits in natural images with unsupervised feature learning," in *NIPS workshop on deep learning and unsupervised feature learning*, vol. 2011, no. 2, 2011, p. 5.

[13] A. Krizhevsky and G. Hinton, "Learning multiple layers of features from tiny images," 2009.

[14] M. E. Nilsback and A. Zisserman, "Automated flower classification over a large number of classes," in *2008 Sixth Indian Conference on Computer Vision, Graphics Image Processing*, Dec 2008, pp. 722–729.

[15] H. Xiao, K. Rasul, and R. Vollgraf. (2017) Fashion-mnist: a novel image dataset for benchmarking machine learning algorithms.

[16] L. Bossard, M. Guillaumin, and L. Van Gool, "Food-101 – mining discriminative components with random forests," in *Computer Vision – ECCV 2014*, D. Fleet, T. Pajdla, B. Schiele, and T. Tuytelaars, Eds. Cham: Springer International Publishing, 2014, pp. 446–461.

[17] A. Coates, A. Ng, and H. Lee, "An analysis of single-layer networks in unsupervised feature learning," in *Proceedings of the Fourteenth International Conference on Artificial Intelligence and Statistics*, ser. Proceedings of Machine Learning Research, G. Gordon, D. Dunson, and M. Dudík, Eds., vol. 15. Fort Lauderdale, FL, USA: PMLR, 11–13 Apr 2011, pp. 215–223. [Online]. Available: http://proceedings.mlr.press/v15/coates11a.html

[18] M. Cimpoi, S. Maji, I. Kokkinos, S. Mohamed, and A. Vedaldi, "Describing textures in the wild," in *Proceedings of the 2014 IEEE Conference on Computer Vision and Pattern Recognition*, ser. CVPR '14. Washington, DC, USA: IEEE Computer Society, 2014, pp. 3606–3613. [Online]. Available: http://dx.doi.org/10.1109/CVPR.2014.461

[19] A. Quattoni and A. Torralba, "Recognizing indoor scenes,"

in *2009 IEEE Conference on Computer Vision and Pattern Recognition*, June 2009, pp. 413–420.

[20] B. Zhou, A. Lapedriza, A. Khosla, A. Oliva, and A. Torralba, "Places: A 10 million image database for scene recognition," *IEEE Transactions on Pattern Analysis and Machine Intelligence*, 2017.

[21] I. Goodfellow, Y. Bengio, A. Courville, and Y. Bengio, *Deep learning*. MIT press Cambridge, 2016, vol. 1.

[22] D. Garcia-Gasulla, A. Vilalta, F. Parés, J. Moreno, E. Ayguadé, J. Labarta, U. Cortés, and T. Suzumura, "An out-of-the-box full-network embedding for convolutional neural networks," *CoRR*, vol. abs/1705.07706, 2017. [Online]. Available: http://arxiv.org/abs/1705.07706

[23] P. J. Rousseeuw, "Silhouettes: a graphical aid to the interpretation and validation of cluster analysis," *Journal of computational and applied mathematics*, vol. 20, pp. 53–65, 1987.

[24] K. He, X. Zhang, S. Ren, and J. Sun, "Deep residual learning for image recognition," in *Proceedings of the IEEE conference on computer vision and pattern recognition*, 2016, pp. 770–778.

[25] J. Deng, W. Dong, R. Socher, L.-J. Li, K. Li, and L. Fei-Fei, "Imagenet: A large-scale hierarchical image database," in *IEEE CVPR*, 2009, pp. 248–255.

[26] Z. Wang, A. C. Bovik, H. R. Sheikh, and E. P. Simoncelli, "Image quality assessment: from error visibility to structural similarity," *IEEE Transactions on Image Processing*, vol. 13, no. 4, pp. 600–612, April 2004.

[27] N. X. Vinh, J. Epps, and J. Bailey, "Information theoretic measures for clusterings comparison: Variants, properties, normalization and correction for chance," *Journal of Machine Learning Research*, vol. 11, no. Oct, pp. 2837–2854, 2010.

[28] L. Hubert and P. Arabie, "Comparing partitions," *Journal of classification*, vol. 2, no. 1, pp. 193–218, 1985.

[29] A. Rosenberg and J. Hirschberg, "V-measure: A conditional entropy-based external cluster evaluation measure," in *Proceedings of the 2007 joint conference on empirical methods in natural language processing and computational natural language learning (EMNLP-CoNLL)*, 2007.

[30] C.-Y. Lee, S. Xie, P. Gallagher, Z. Zhang, and Z. Tu, "Deeply-supervised nets," in *Artificial Intelligence and Statistics*, 2015, pp. 562–570.

[31] T. Tieleman and G. Hinton, "Lecture 6.5-rmsprop, coursera: Neural networks for machine learning," *University of Toronto, Technical Report*, 2012.

[32] K. He, X. Zhang, S. Ren, and J. Sun, "Delving deep into rectifiers: Surpassing human-level performance on imagenet classification," in *Proceedings of the IEEE international conference on computer vision*, 2015, pp. 1026–1034.